Further Discussions About Drying

W. Snyder, C. Whitehouse, J. Markee

1.0 ABSTRACT

At the 2018 ICI Fall Technical Conference, three foundries presented papers on drying data gathered at their foundries. These papers resulted in a lot of discussion about how the level of dryness impacts shell strength. This year, additional work was planned to continue the discussion around shell drying. In this paper, a mold dryness measurement system was used to provide a more complete understanding of shell properties at various levels of dryness. Three levels of relative shell humidity prior to re-dipping used and a number of shell properties were measured including burst strength, permeability, and the four standard test conditions: green, hot/wet (boiled), fired tested hot and fired cooled to ambient (fired/cold).

On a parallel path, DePuy Synthes gathered additional data around the level of dryness in the mold and correlated this data to casting quality, which will be presented in a separate paper at the 66th Technical Conference. From this data, it is hoped that foundries will be able to better understand how mold dryness impacts shell strength and casting quality.

2.0 BACKGROUND

The level of mold dryness required to make a good casting is a question which is frequently asked by an investment casting foundry. Many papers have addressed different aspects of shell drying over the years. Three papers were presented at last-year's 65th Technical Conference on the topic of drying. Brienza [1] attempted to establish a relationship between shell properties and the degree of dryness. A review of shell temperature, shell relative humidity and electrical conductivity due to the presence of water remaining in the shell was made and compared to shell modulus of rupture data. It was found that the greater the temperature recovery, the higher the green MOR. However, it was pointed out that a relationship between the dryness and the amount of water remaining in the mold was not established. Oyervides [2] studied the dryness of internal passageways also using relative humidity. This paper concluded that there was no apparent impact on shell quality within a range of 60% to 80% relative humidity in the shell. Tella [3] studied shell dryness at the wax surface and exterior shell surface and presented data showing the change in relative humidity from these locations during the DePuy drying cycle.

Many other papers have been presented over the years on drying. Snow [4] shared extensive data on the effect of air temperature, humidity and air velocity upon drying time using shell weight changes due to evaporation as well as the resultant shell strengths. Leyland [5] presented further extensive data on shell drying and suggested that "… water in the gel structure cannot flow freely to the surface" and that the shell pore structure further complicates drying due to with the presence of colloidal gel as the water evaporates.

Markee [6] noted that as the level of complexity of the molds increases, ensuring the inside of the mold is dry enough for the next layer or prior to dewax is critical. This paper indicated that using temperature as a method for measuring mold dryness in the inner passageways may lead to inadequate data. Further, that without proper air movement, the relative humidity of these areas may reach 100%, drying will then stop, and the temperature will begin to climb towards ambient. As a result, % RH was recommended as the best method for measuring mold dryness on the inner passageways of a mold.

3.0 EXPERIMENTAL

3.1 Materials and Equipment

3M™ WDS2 Fused Silica Advanced Shell System, Nalco's small particle 1130 colloidal silica, and 3M™ HP Latex were all sourced for slurry making as shown below in Table 1.

	Wt(g)
WDS2 flour	13500
1130 colloidal	4883
DI-H2O	600
HP Latex	501
Antifoam	10
Total	19494
%SiO2	24.4%
%latex	8.4%

Table 1. Slurry Formula.

Slurry was high sheared for a total of 30 minutes and allowed to cream in overnight (18 hours) in a large rotating Nalgene jug. Slurry creamed in at 20 seconds as measured on a Zahn EZ #5 dip cup.

Mold dryness was measured using Key Process Innovation's KPI-DRI™ system. At the desired location, a digital sensor with a waterproof, breathable membrane measures temperature and relative humidity.

Three levels of shell dryness were used in this study: 75%RH, 60%RH and 45%RH. Once these degrees of dryness were achieved in the shells after each dip, a subsequent dip was applied. Shell conditions were then measured after an 18-hrs final dry time was used. Room temperature and humidity as well as shell temperature and humidity were measured.

3.2 Procedures and Sample Preparation

Standard 1"x 0.25" x 13" steel bars were used for MOR testing. 3/4" schedule 40 inner diameter cold PVC pipes were used for shell building for permeability testing per the method discussed by Snyder [7]. Lastly 4" x 4" x 0.25" wax plates were used to provide data on slurry draining and shell building. Substrates were first coated in Johnson's Paste wax followed by a dip in surfactant and then allowed to dry.

A five-dip shell was made for these tests. First dip in WDS2 was stuccoed with 50x100 fused silica. The second, third and fourth dips were stuccoed in 30x50 fused silica. The last dip was a seal coat.

Shell drying was performed in a small 5'x 8' closed room with its own air conditioning and resistance heating unit. A programmable controller is used to control the temperature while a portable Dri-Eaz Model Revolution LGR dehumidifier is used to control the humidity with use of a setpoint controller. No additional humidifier was used as humidity in eastern Tennessee is typically 50% or greater at the time of year of in which this test was performed. This did result in a slight loss of humidity control one day as an unexpected dry front came through which will be mentioned later. Air is kept turbulent with use of two opposing and wall mounted oscillating fans which provide velocities typically between 100 to 800 ft/ min.

The dry room was controlled to 72±2°F. For consistency, the room humidity was dropped to 40%RH for all shell drying conditions. Cold rolled steel MOR bars 1" x 1/8" x 13" were

used for MOR shell building and for mounting to the KPI-DRI sensor system (shown below in Photos 1 and 2).

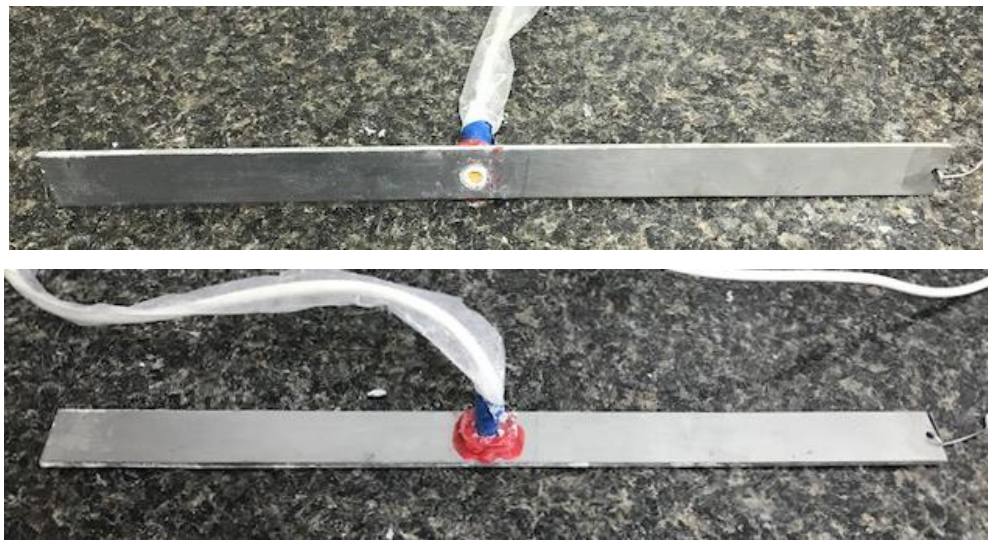

Photo 1. Two Images of MOR Bar Equipped with KPI-DRI Sensor.

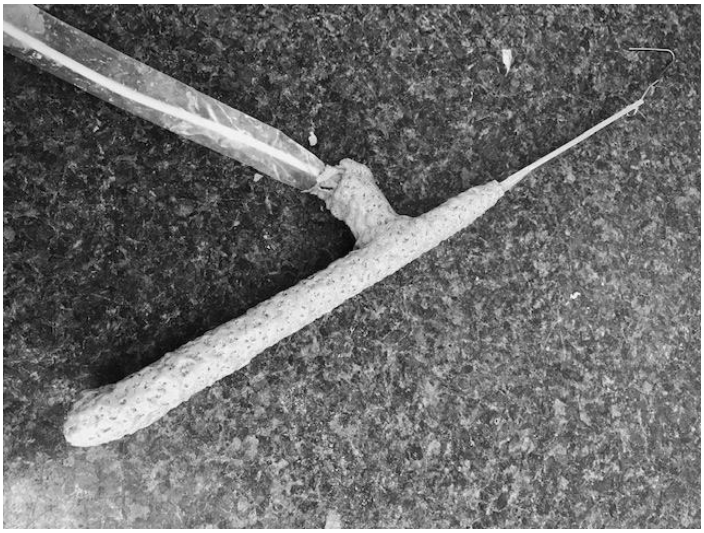

Photo 2. Image of Shelled MOR Bar with KPI-DRI™ Sensor.

The complete shell dryness monitoring system from KPI is shown below in Photo 3.

Photo 3. KPI-DRI™ Shell Dryness Monitoring System.

MOR testing was performed using an Instron 3342 with a 500N/ 112 lbs. load cell. A cross head speed of 0.05"/min along with a two-inch span is used for testing. The thickness of the bar at the break is measured in six locations across the break, three on each side of the break; the width is measured twice and averaged. Shells were removed from the PVC pipes and cut into 6" lengths for permeability and burst testing.

3.0 RESULTS AND DISCUSSION

3.1 Shell Conditions During Drying

The entire shell dry condition for 75%RH is shown below in Fig. 1. Temperature is shown on the left axis in orange and relative humidity is shown on the right axis in blue. Both the room condition and the shell condition for both variables is shown, resulting in four curves total. From the figure it is clear that room temperature condition was well maintained and was steady. Shell temperature (in light orange) was shown to vary with evaporative cooling reaching a minimum of 57-60°F wet-bulb temperature. Humidity in the room started at 50%RH initially but dropped to a steady 40%RH eventually. Shell humidity/ dryness was seen to vary from 60% to 95% as measured with the KPI-DRI™ system.

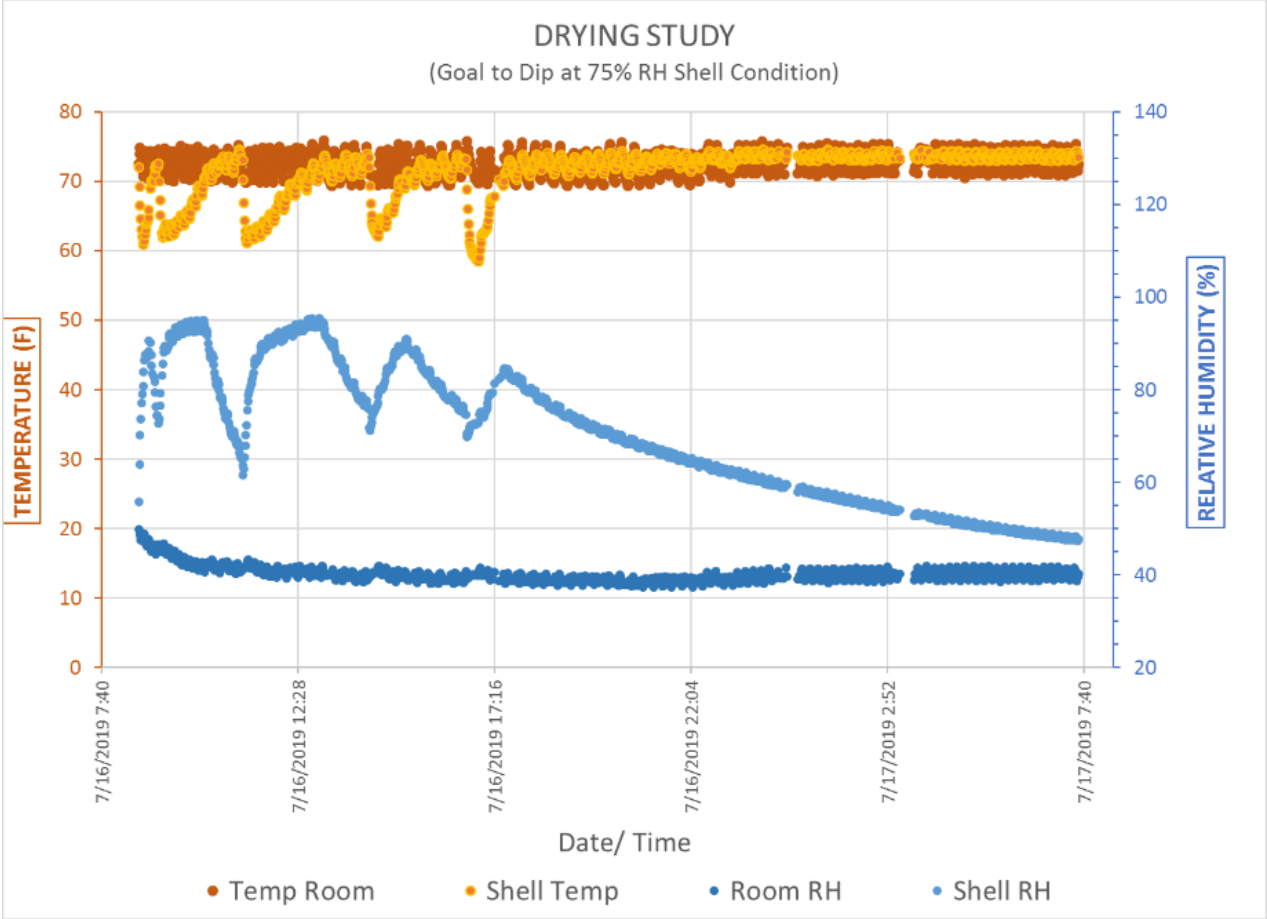

Fig. 1. 75% RH Dryness Level for Dipping.

Below in Fig. 2 the drying condition of shells controlled to 60%RH or higher is shown. Room and shell temperatures are essentially identical to those of the 75% RH condition above. Room humidity was better controlled initially and throughout the entire drying study. Shell humidity/ dryness varied from 60% to 95% between dips.

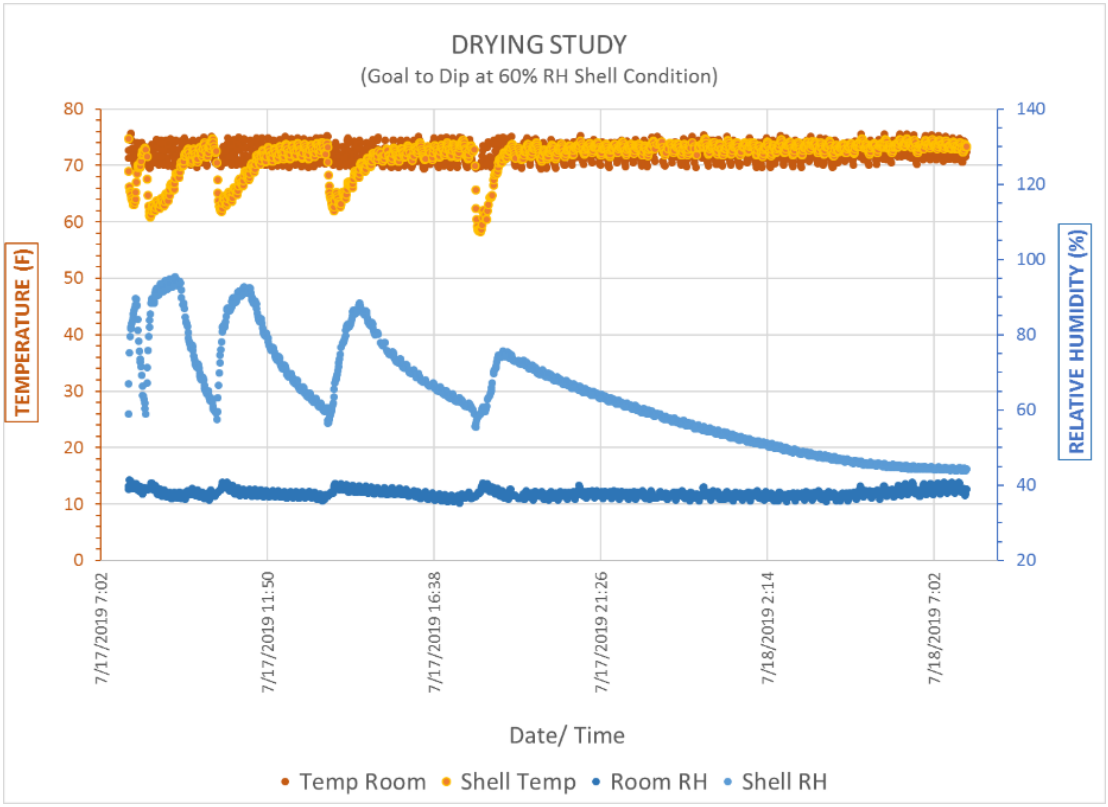

Fig. 2. 60% RH Dryness Level for Dipping.

The most completely dried shell condition is shown below in Fig. 3. Room and shell temperatures were not well controlled during the first day. An unusually dry weather condition rolled through northeast Tennessee which caused much consternation and tweaking to try to maintain the room conditions. As can be seen, it was not terribly successful. However, the temperature and humidity controls were re-established and drying continued as normal. Shell humidity was overall controlled between 45%RH and 95%RH.

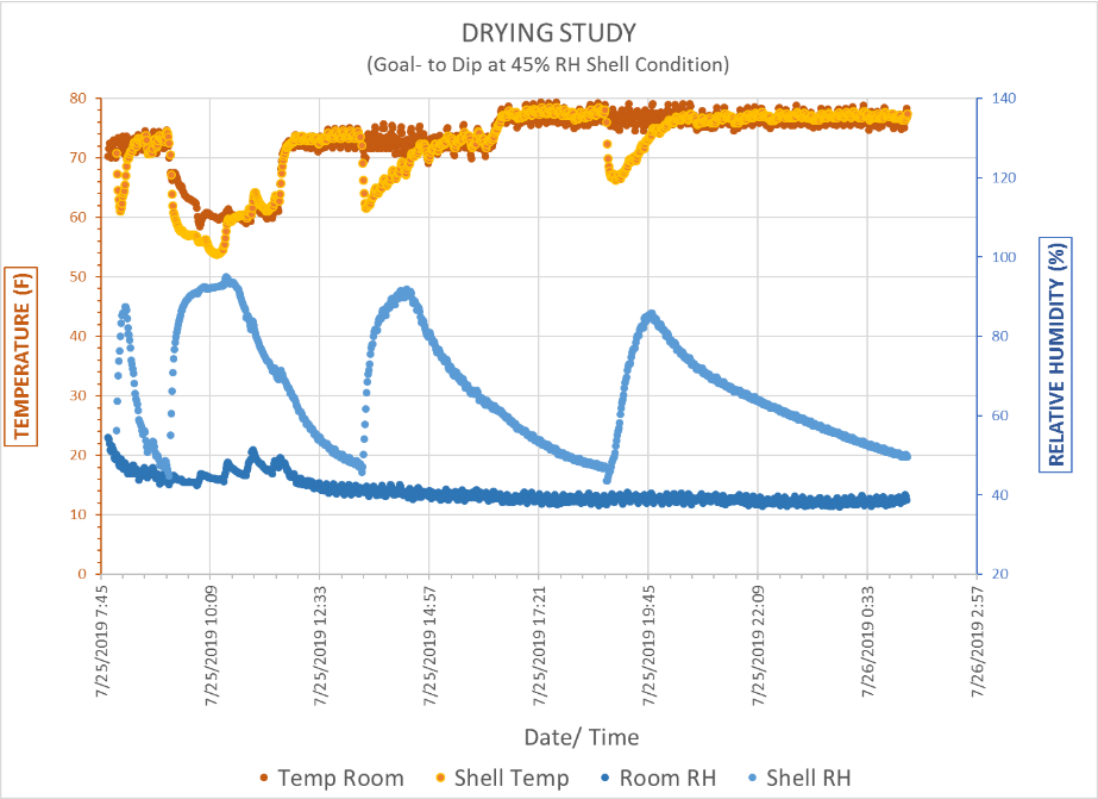

Fig. 3. 45% RH Dryness Level for Dipping.

One interesting point is that even when dipping to 75% RH, the recovery temperature is nearly 100%. This suggests using relative humidity as a dryness indicator on feature-less or simple geometries may not be necessary as it correlates closely with temperature recovery, see Fig. 4 below.

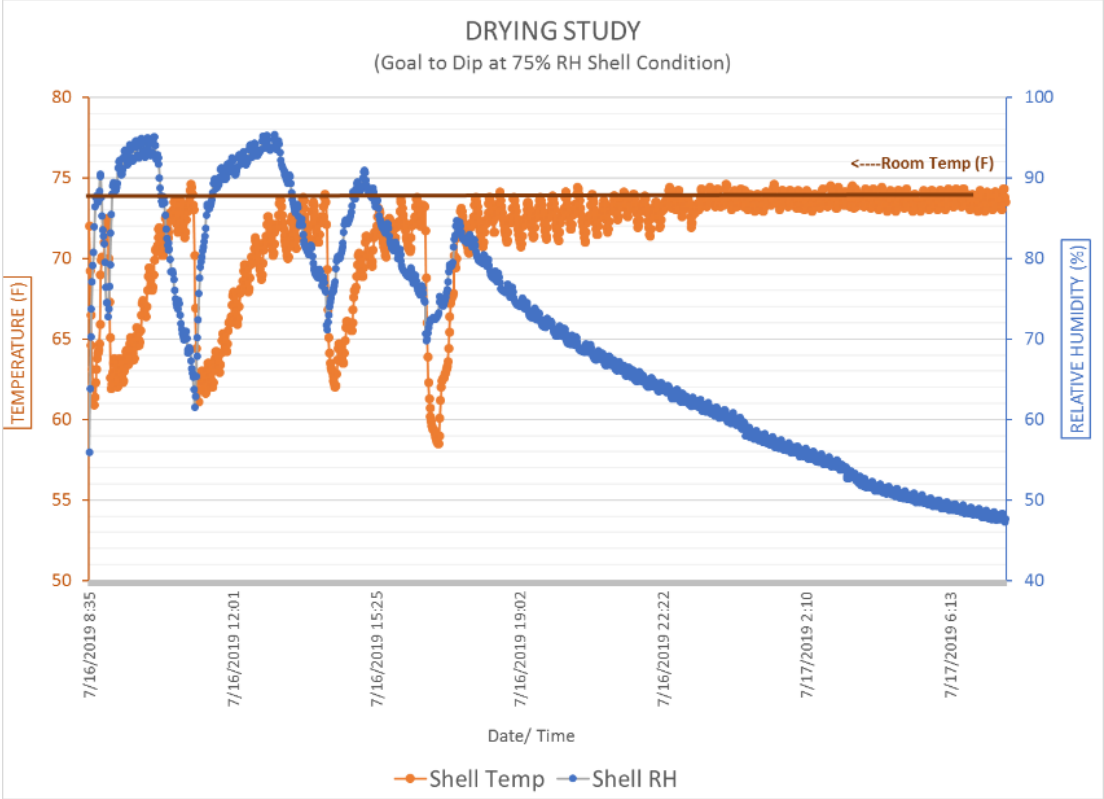

Fig. 4. Shell Temperature and Humidity – 75% RH Condition

3.2 Shell Properties

3.2.1 Shell Thickness

Thickness of shells were measured on both the pipe sections and the MOR bar sections (Figs 5 and 6) and extreme uniformity was seen across all substrates.

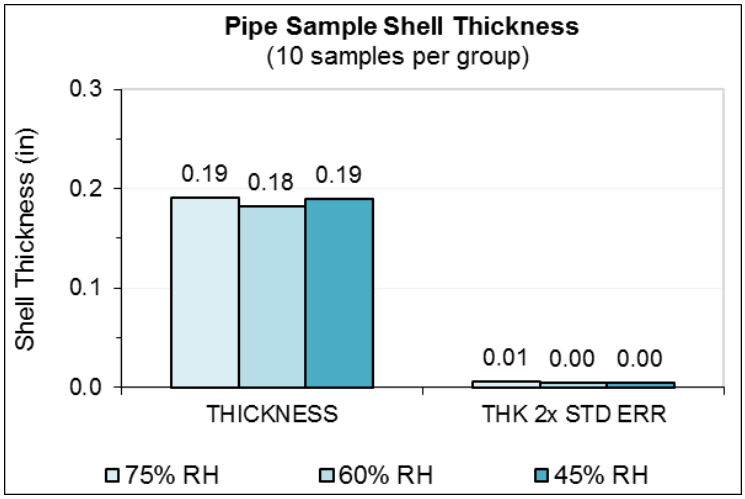

Fig. 5. Shell Thickness Measured from Pipes.

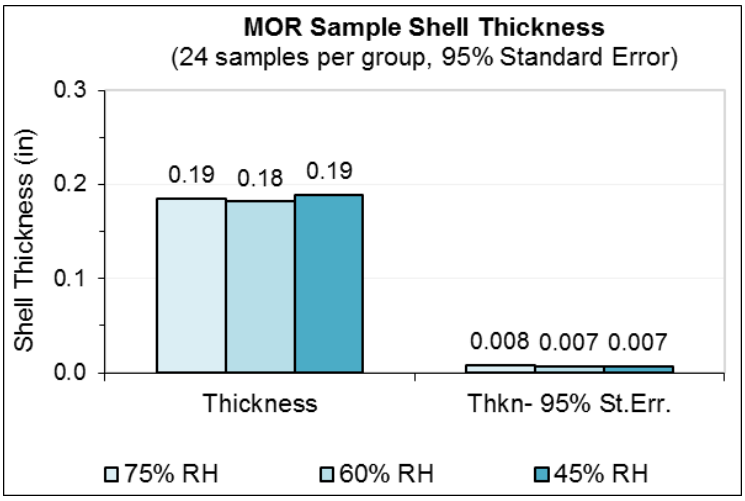

Fig. 6. Shell Thickness Measured from MOR Bars.

4.2.2 Shell Permeability

After pipe sections were measured for thickness, the pipe shells were measured for shell permeability per the Snyder method [7]. Similar to shell thickness performance above, no average discernable difference in permeability was recorded. Results are depicted below in Fig. 7.

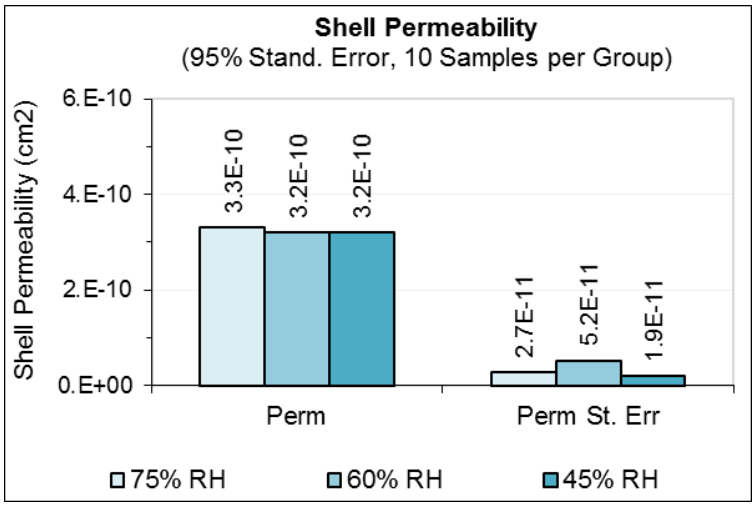

Fig. 7. Shell Permeability Measured in the Green State.

4.2.3 Maximum Tangential Stress Results (Burst Test)

Burst strength of the shell was next measured and is shown below in Fig. 8. Here again, consistent performance was measured with respect to the measured error bars.

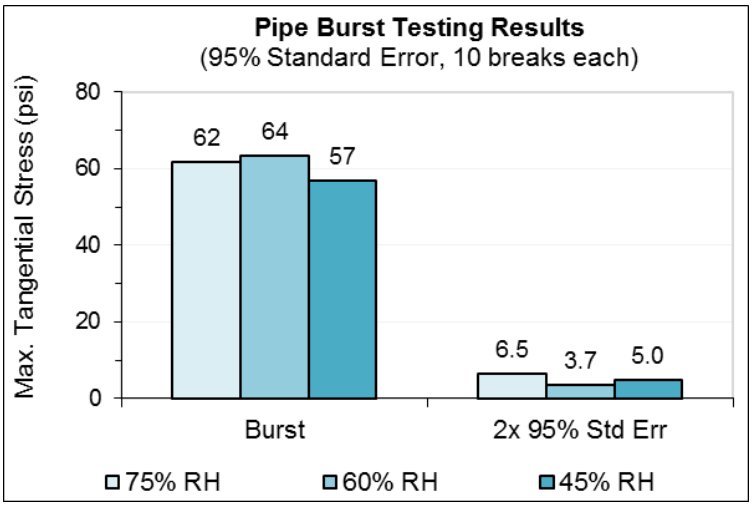

Fig. 8. Shell Maximum Tangential Strength Measured in the Boiled State.

4.2.4 Green Shell Properties

Strength of the shell was measured in the dried, or green state, from MOR bar sections. After the final dry after seal dip of 18 hrs., shells were taken and broken for these results. Strength is depicted below in Fig. 9 where again shell performance was largely unaffected by measured degree of shell dryness. Considering the measured standard error bars, no discernable difference was seen.

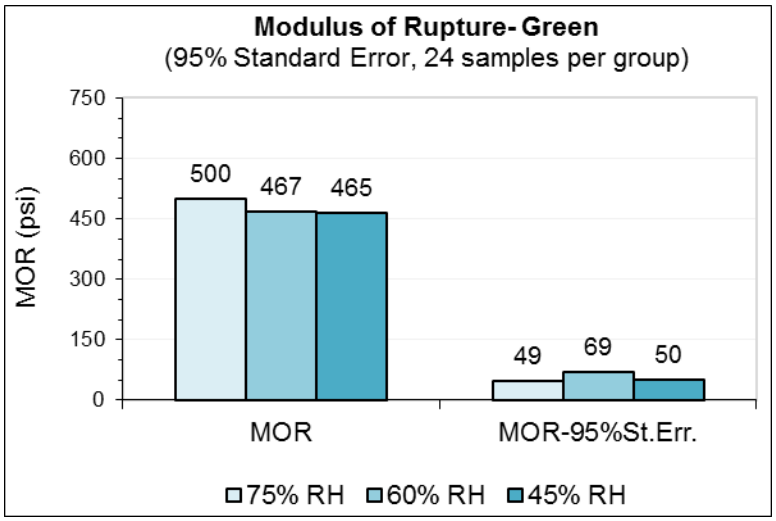

Fig. 9. Green Shell Strength.

Shell rigidity is depicted in Fig. 10 below in the green state. Again, no discernable difference was noted.

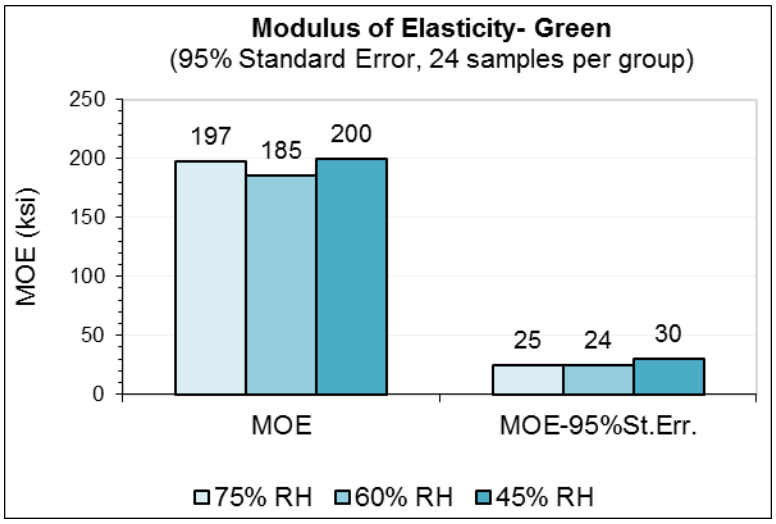

Fig. 10. Green Shell Rigidity.

Load required for shell failure is next depicted below in Fig. 11 where again, respective of the measured errors, no true discernable difference in shell failure loads is seen.

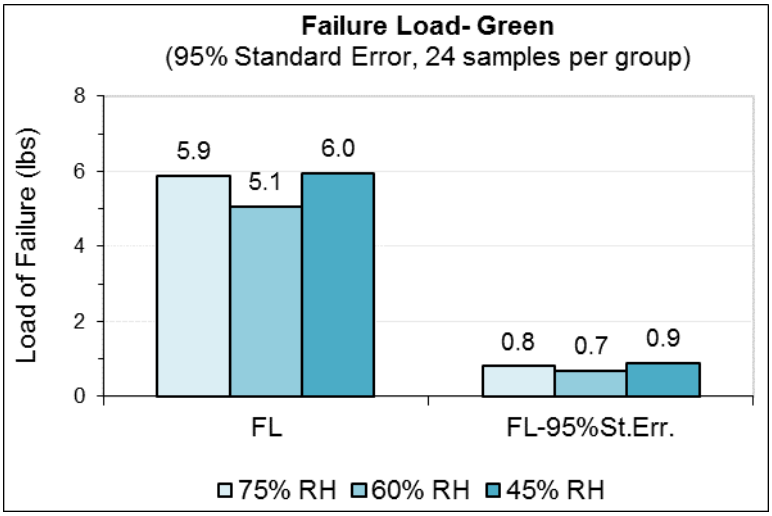

Fig. 11. Green Shell Failure Load.

Lastly, the fracture index in the green state is shown below in Fig. 12. As expected, no trends and no true differences were seen.

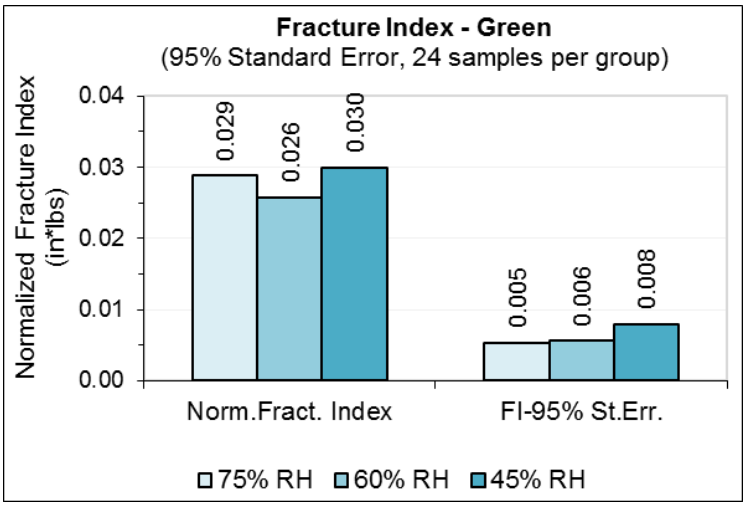

Fig. 12. Green Shell Fracture Index.

4.2.5 Hot/Wet (Boiled) Shell Properties

After a final dry of 18 hrs., shells were boiled for 15 minutes and taken from the water and broken immediately, one break at a time, for these measurements. The 75%RH shells did demonstrate a greater strength than the other two more dried groups. This difference is greater than the measured error bars; however, with no clear trend shown it is difficult to draw any possible conclusions here (Fig. 13).

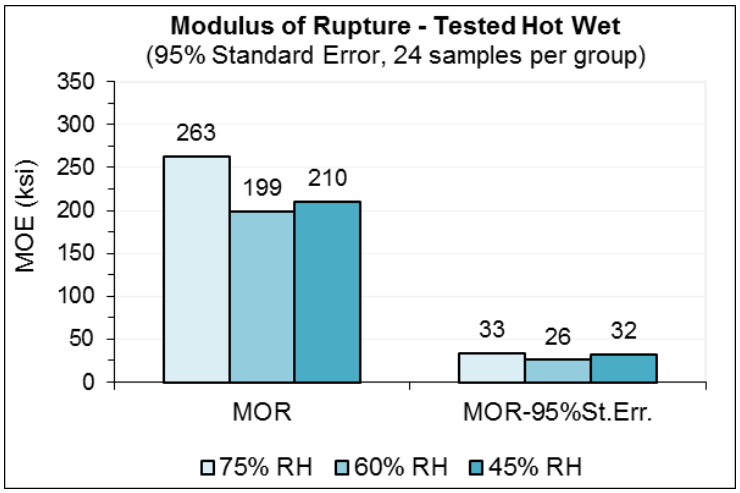

Fig. 13. Hot/wet Shell Strength.

Rigidity of the shells in this boiled and latex softened state is shown below in Fig. 14. Perhaps a slight increasing trend in stiffness is suggested below with a greater degree of shell dryness between dips. No true difference between 75 and 60% RH exists when considering the measured errors, but a numerical trend may exist.

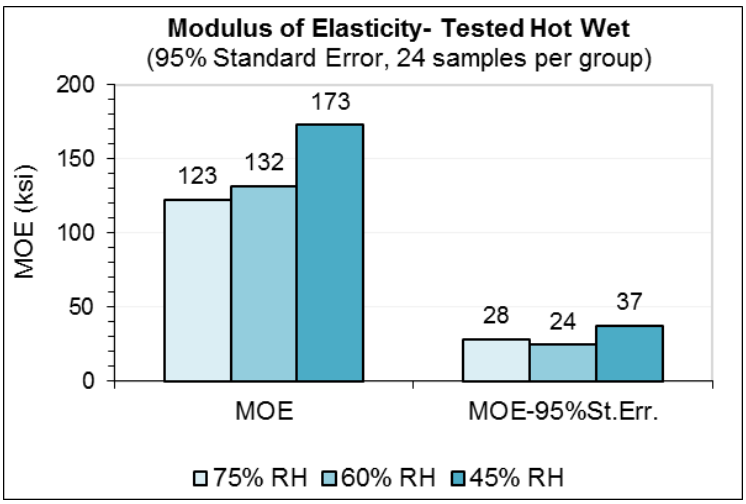

Fig. 14. Hot/wet Shell Rigidity.

Load required for shell breakage in this boiled state is shown below in Fig. 15 where the greatest load was held by the 75% RH sample group. Performance difference here was greater than the measured errors. No difference is shown for the two more dry group averages of 60 and 45% RH.

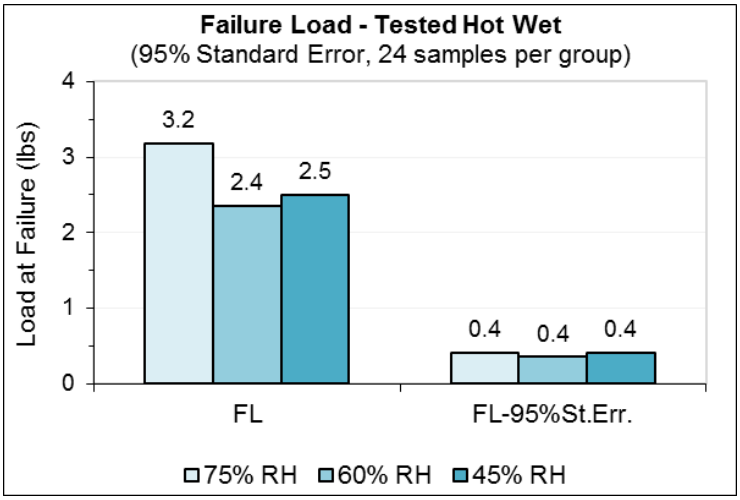

Fig. 15. Load of Fracture in the Hot/wet State.

Fracture index in this state is depicted below in Fig. 16 where again the less dry between dips shell demonstrated best performance. Again, no differnce was realized between the two more dried shell group averages.

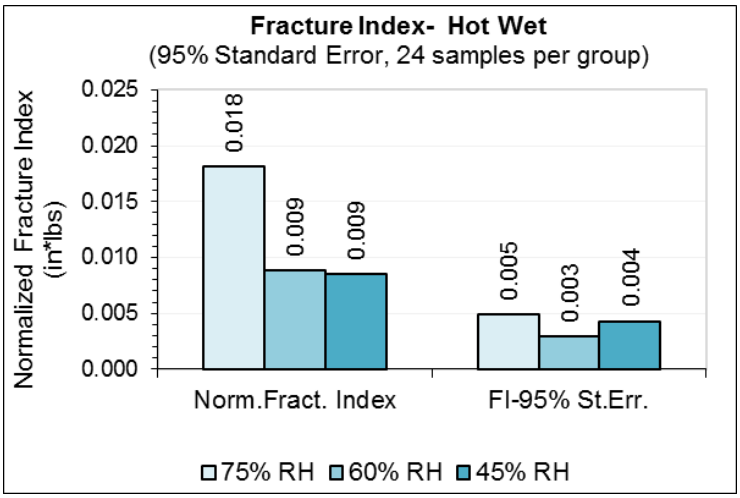

Fig. 16. Fracture Index in the Hot/wet State.

4.2.6 Fired/ Hot Shell Properties

Shell sections were next tested in a fired state where samples were held at 2000°F for a minimum of two hours. One sample at a time was taken out and broken immediately in the Instron while still glowing 'orange/red-hot'. This state is an attempt to duplicate shell condition in the 'metal poured' state. Strength results are shown below in Fig. 17 where no difference was seen between group averages.

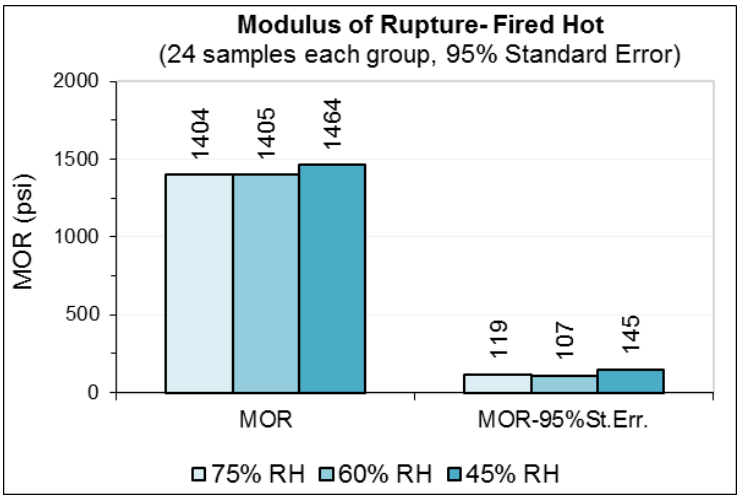

Fig. 17. Shell Strength in Fired and Hot State.

Shell stiffness in this state is shown below in Fig. 18. Shells from the 60% RH group demonstrated the greatest rigidity in this test; however, the high measured error of this

group introduces uncertainty of a true higher value here. All told, little is seen in this test to suggest any trends.

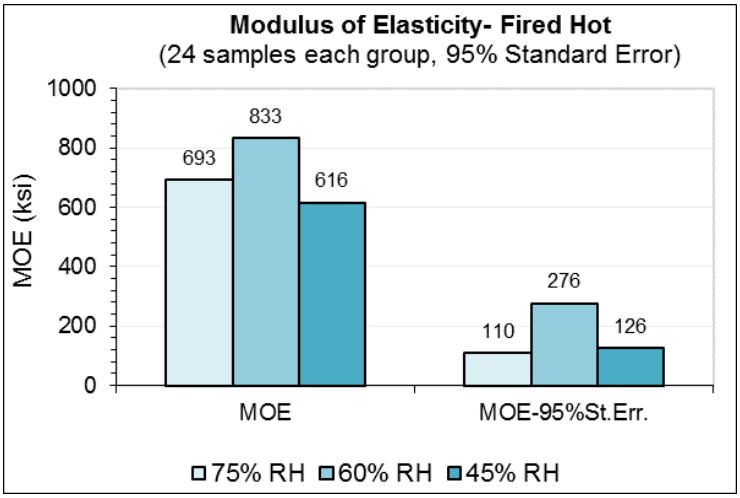

Fig. 18. Shell Rigidity in the Fired and Hot State.

Failure load in this hot state is shown below in Fig. 19 where when considering measured errors, no difference or trend is seen between groups.

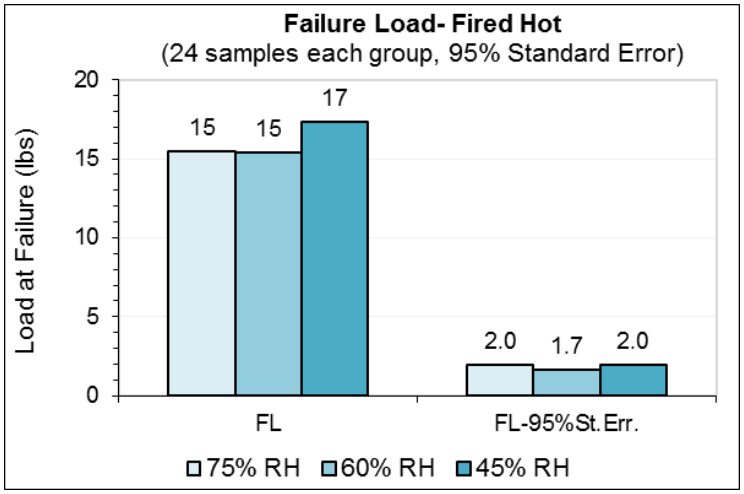

Fig. 19. Shell Load of Failure in the Fired and Hot State.

Shell fracture index was measured and appears below in Fig. 20. Again, differences between groups here is only slighty greater than the measured errors and no trend is seen in these three groups.

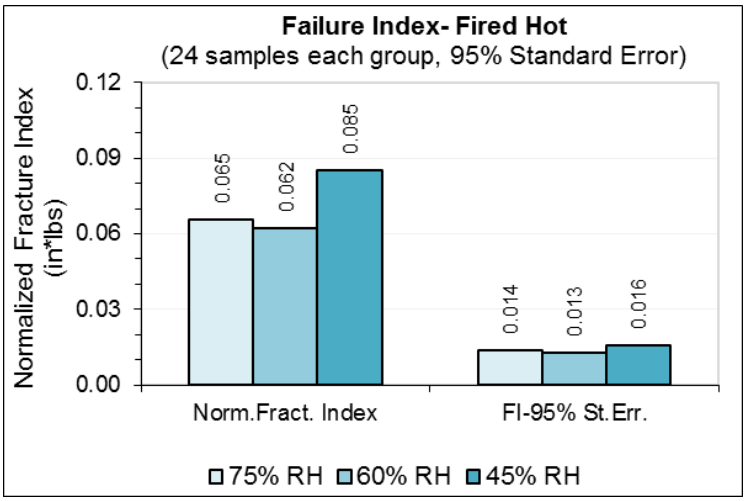

Fig. 20. Fracture Index in the Fired and Hot State.

4.2.7 Fired/ Cold Shell Properties

Shells were tested next in the fired and cooled to ambient state. This best represents the shell 'knock-out' condition where reduced strengths are most desired. Averages of the groups shows the worst performance was recorded for the 75% RH group; however, this group also had the greatest variation in the individual measurements and has the greatest overall standard error. With this factored into the comparison, no difference is realized in this figure below.

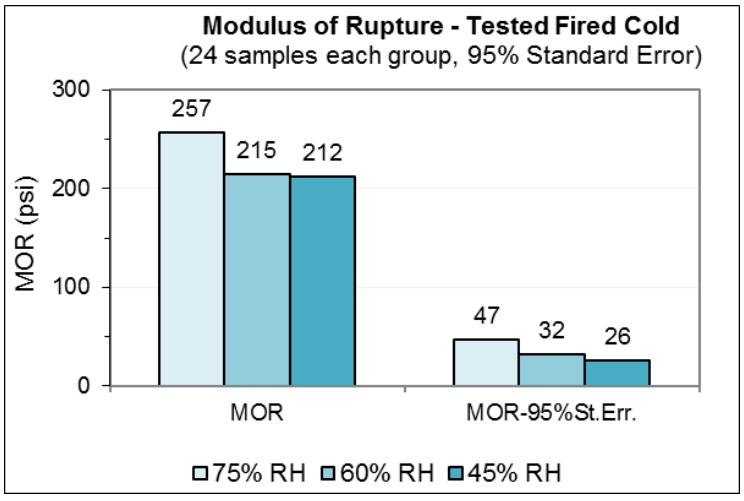

Fig. 21. Fired Measured Cold Shell Strength.

Fired and cold shell rigidity is next shown in Fig. 22 below. The two least dry conditions demonstrate nearly identical performance. The most dry shell group does depict a significant and lower rigidity, especially when considering the error bars.

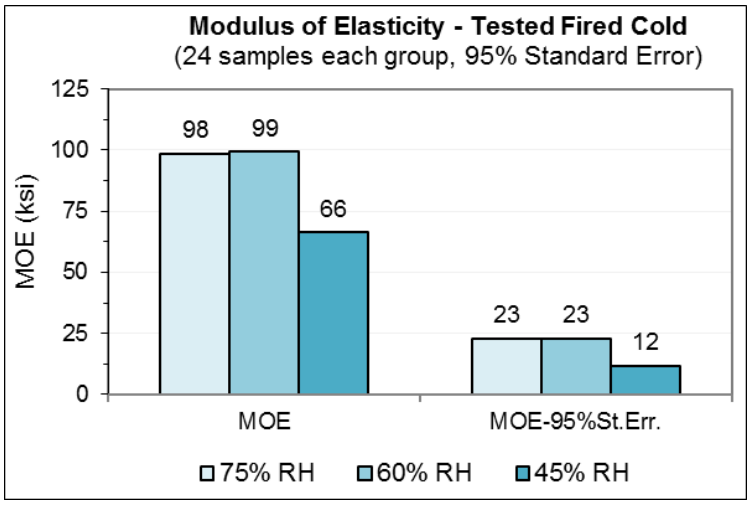

Fig. 22. Fired Measured Cold Shell Rigidity.

Shell load of failure in this knockout state is shown below in Fig. 23. Yet again, differences between group averages is within the measured errors and no trend is apparent.

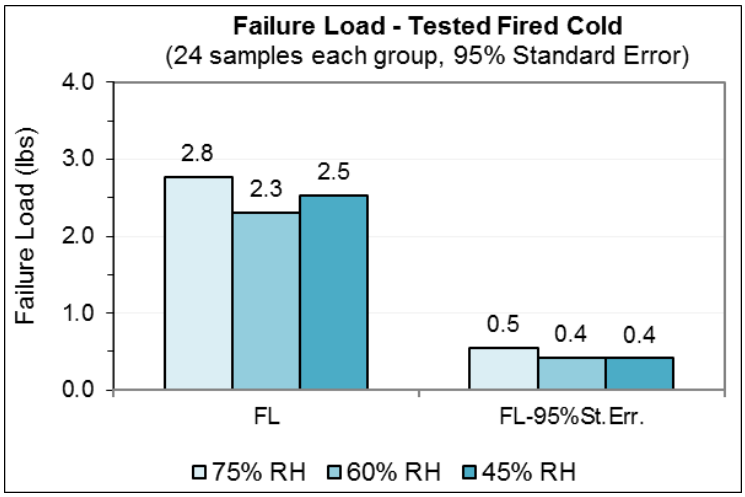

Fig. 23. Fired Measured Cold Shell Failure Load.

Fracture index in this state is shown below in Fig. 24. Measured errors here make any difference between groups here difficult to discern, especially without any apparent trend in the data.

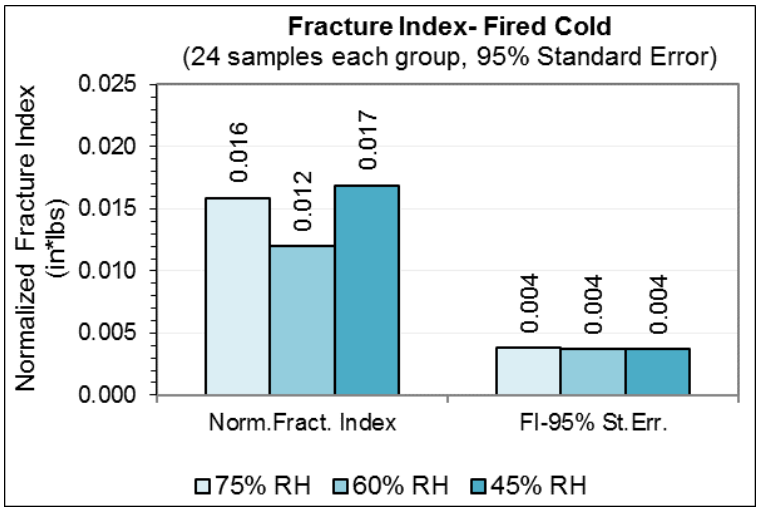

Fig. 24. Fired Measured Cold Shell Fracture Index.

5.0 CONCLUSIONS:

5.1 Differing degrees of shell dryness were achieved but no obvious trends in shell performance in any of the test states were clear.

5.2 This data does show that the temperature reached nearly 100% recovery, even when dipping at 75% RH. Since this is the highest moisture content of the tests, it could be that the data didn't show any differences in shell strength because all molds reached nearly 100% temperature recovery with turbulent air flow.

5.3 Additional tests are being planned to shed more light on shell strength and shell humidity.

6.0 REFERENCES:

1. M. Brienza, et.al. "Intercoat Drying and Shell Properties", 65th Annual Technical Meeting of the Investment Casting Institute, 2018, pp 6:8-20.
2. M. Oyervides, "A Brief Look into MetalTek Wisconsin Investcast's Shell Drying Process", 65th Annual Technical Meeting of the Investment Casting Institute, 2018, pp 6:1-7.
3. R. Tella, et.al. "DePuy Synthes kpi-dry™ Case Study", 65th Annual Technical Meeting of the Investment Casting Institute, 2018, pp 6:21-24.
4. J. Snow, et.al. "Shell Drying- Water Based", 46th Annual Technical Meeting of the Investment Casting Institute, 1998, pp 8:1-30.

5. S. Leyland, et.al. “Implementation of a Water Based shell Mould Investment Casting Process,” 9th Annual World Conference on Investment Castings, 1996, pp: 23.
6. J. Markee, “A New Method for Measuring Dryness during the Shell Building Process,” 59th Annual Technical Meeting of the Investment Casting Institute, 2012, pp 7:1-9,
7. B. Snyder, et.al. “A New Combination Shell Strength and Permeability Test”, 51st Annual Technical Meeting of the Investment Castings Institute, 2003, pp 11:1- 26.